논 문
60-5-7

극수/슬롯수 조합에 따른 Radial Vibration Force 고려한 매입자석 동기모터 특성 연구

Study on Machine Characteristics in Interior Permanent Magnet Synchronous Motor According to Pole/Slot Combinations with Radial Vibration Force Consideration

방 량* · 이 수 진* · 이 병 화* · 홍 정 표†
(Liang Fang · Su-Jin Lee · Byeong-Hwa Lee · Jung-Pyo Hong)

Abstract - This paper presents a comparative study on motor characteristics with specific consideration of radial vibration force in interior permanent magnet synchronous motors (IPMSM) according to pole/slot combinations. Three IPMSM models, 16-pole/15-slot design, 16-pole/18-slot design and 16-pole/24-slot design are built, in which 16-pole/15-slot and 16-pole/18-slot designs provide high winding factor and 16-pole/24-slot design is known as a general pole/slot combination. By coupling finite element analysis (FEA) with equivalent circuit method, motor characteristics, back electro-motive force (Back-EMF), inductances, cogging torque, etc. as well as machine output performances are analyzed and compared. The radial vibration force (RVF) distribution in air gap causing stator vibration and noise is interested. It is expected that this study help with appropriate choice of pole/slot combination in IPMSM design.

Key Words : FEM, IPMSM, Motor characteristics, Pole/slot combination, Radial vibration forces

1. Introduction

Permanent magnet machines have wide applications because they offer excellent maintainability, controllability, and environmental endurance while providing high-efficiency operation with high power factor [1]. Especially, the interior permanent magnet synchronous machine (IPMSM) produces higher power density since it can utilize both magnetic torque and reluctance torque, and provides wide speed range by field weakening control. Recently, more and more interests are attracted on IPMSM researches.

It is known that the choice of pole/slot combination in IPMSM design will significantly affects machine characteristics as well as winding configuration. The winding layouts of motor generally are divided into concentrated winding and distributed winding. The concentrated winding design has advantages of short end-coil and simple structure suitable for high volume automated manufacturing in comparison with the distributed winding [2], however, it has problems of general lower winding factor, higher torque ripple and cogging torque than distributed winding design, which need more attentions to be paid in detail design.

However, by choosing an appropriate pole/slot combinations in concentrated winding design, the winding factor, torque ripple and cogging torque can be significantly improved before machine detailed design. On the other hand, some motor characteristics also can be affected undesirable. In some fractional pole/slot combinations, if the machine has parallel circuits, that induces circulating current and results in increasing of electric noises and additional copper loss, which should be considered seriously in motor design.

Noise and vibration are important characteristics must be concerned in the IPMSM design. As one of important souse, the radial force vibration (RVF) should be investigated in designing stage. In some design cases of pole/slot combinations, unbalanced RVF occurs and damages bearings.

This study is concern to choose an appropriate pole/slot combination under trade-off of IPMSM characteristics and specific consideration of RVF distribution in air gap. Among various pole numbers, 16-pole (16p) IPM design is chosen to build analysis models with conventional unbalanced combinations, 15-slot (15s), 18-slot (18s), as well as balanced combination 24-slot (24s), respectively. The finite element analysis (FEA) coupled with equivalent circuit method is used for calculating machine characteristics.

* 정 회 원 : 한양대 공대 자동차공학과 박사과정
† 교신저자, 펠로우회원 : 한양대 공대 자동차공학과 교수
E-mail : hongjp@hanyang.ac.kr
접수일자 : 2011년 1월 1일
최종완료 : 2011년 4월 2일

2. Study Models, Characteristics Analysis and Results Comparison

2.1 Models Specification

In this study, three IPMSM models are built, 16p/15s model, 16p/18s model and 16p/24s model. TABLE. I lists their basic specifications and Fig. 1 shows their different stator structures and identical rotor geometries, in which their yoke and tooth width are designed to have identical filling factor of coil with identical current density for each model without detailed design.

Winding configuration of one phase in each model are shown in Fig. 2. With choosing different pole/slot combination, the different winding configuration leads to the winding factor variation, as TABLE. II gives [2], in which 15-slot, 18-slot, and 24-slot with 16-pole are calculated as 0.951, 0.931, 0.866, respectively [5].

Another important aspect is circulating current phenomenon, when parallel circuit is adopted. Due to different slot pitch in electrical degree, the angular positions of each coil of one phase in 15-slot and 18-slot model are different. Therefore, circulating currents will occur in 15-slot and 18-slot model. Circulating currents decreases efficiency and increases electric noise Therefore, parallel circuits should be avoided in 15-slot and 18-slot with 16-pole design. In addition, the 24-slot models can use 1/8 models on the basis of periodicity, while 15-slot does full model and 18-slot does 1/2 model in FEA, which should be aware that the symmetric simple model can save huge computation time in detailed design by FEA.

Table 1 Basic Specification of Study Models

Item	16p/15s model	16p/18s model	16p/24s model
Output Power (kW)	12		
Stator Outer Diameter (mm)	277		
Stack Length (mm)	32		
Air gap Length (mm)	0.8		
Rotor Outer diameter (mm)	200		
Series Turn Per Phase	52		
Parallel Circuit	5	6	8

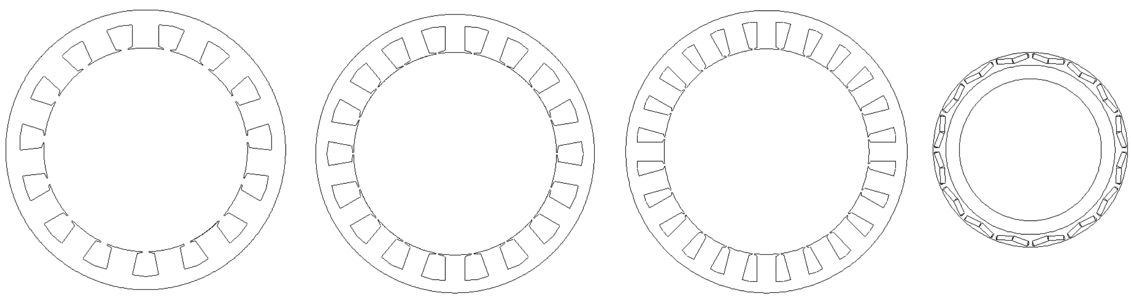

(a) (b) (c) (d)

Fig. 1 Study models of (a). 15-slot stator, (b). 18-slot stator (c). 24-slot stator and (d). 16-pole IPM rotor

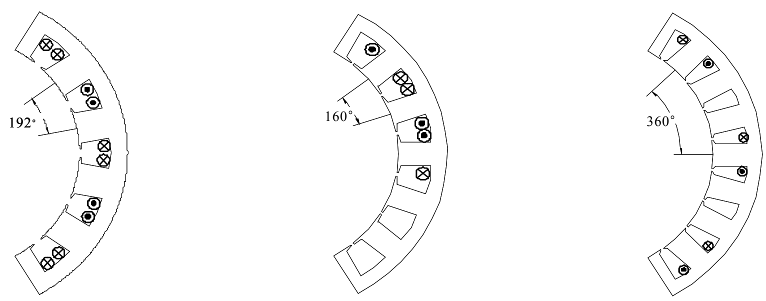

(a) (b) (c)

Fig. 2 Winding configuration of one phase (a). 15-slot stator, (b). 18-slot stator (c). 24-slot stator

Table 2 Winding Factor According to Pole/Slot Combination

Slot number	Pole number				
	8	10	12	14	16
9	0.945	0.945	0.764	0.473	0.175
12	0.866	0.933	-	0.933	0.866
15	0.621	0.866	0.906	0.951	0.951
18	0.543	0.647	0.866	0.902	0.931
21	0.468	0.563	0.521	0.866	0.851
24	-	0.463	-	0.760	0.866

2.2 Analysis Method

In this study, for predicting performance characteristics of IPMSM, an well-accepted d-q axis equivalent circuits method is adopted, particularly the iron core losses consideration is included by using equivalent resistance Rc, as presented in Fig. 3. The mathematical model is given by equations (1), (2), and (3).

Voltage Equation:

$$\begin{bmatrix} V_d \\ V_q \end{bmatrix} = R_a \begin{bmatrix} i_{od} \\ i_{oq} \end{bmatrix} + \left(1 + \frac{R_a}{R_c}\right) \begin{bmatrix} v_{od} \\ v_{oq} \end{bmatrix} + p \begin{bmatrix} L_d & 0 \\ 0 & L_q \end{bmatrix} \begin{bmatrix} i_{od} \\ i_{oq} \end{bmatrix} \quad (1)$$

$$\begin{bmatrix} V_{od} \\ V_{oq} \end{bmatrix} = \begin{bmatrix} 0 & -\omega L_q \\ \omega L_d & 0 \end{bmatrix} \begin{bmatrix} i_{od} \\ i_{oq} \end{bmatrix} + \begin{bmatrix} 0 \\ \omega \Psi_a \end{bmatrix} \quad (2)$$

Torque Equation:

$$T = P_n \{ \Psi_a i_{od} + (L_d - L_q) i_{od} \, i_{oq} \} \quad (3)$$

where, i_d and i_q are d- and q-axis armature current, i_{cd} and i_{cq} are d- and q-axis iron loss current, v_d and v_q are d- and q-axis voltage, R_a is armature winding resistance per phase, R_c is iron loss resistance, Ψ_a is flux linkage by PMs at no-load, L_d and L_q are d- and q-axis inductances, and P_n is number of pole pairs.

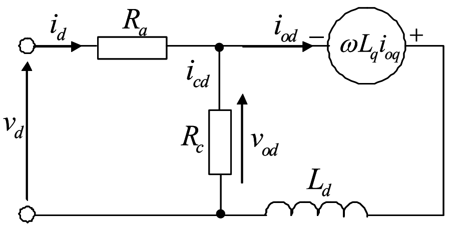

(a) d-axis equivalent circuit

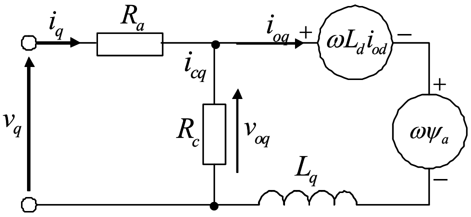

(b) q-axis equivalent circuit

Fig. 3 D-q equivalent circuit model

2.3 Machine Parameters

2.3.1 Back-EMF, THD, Cogging Torque

As a very important machine design parameter, Back-EMF characteristics of three analysis models with identical series turn per phase, are calculated by FEA. Fig. 4 shows comparison of their line-to-line Back-EMF and corresponded THD analysis at 1000[rpm] rotation, in which the 16p/15s model provides the highest fundamental Back-EMF due to high winding factor and with low harmonic components.

Cogging torques among of three models are compared in Fig. 5. The 16p/15s model shows minimum cogging torque among three models due to its large least common multiple of pole/slot numbers.

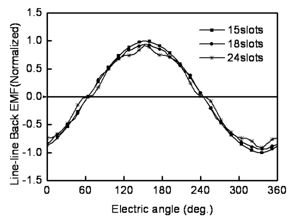

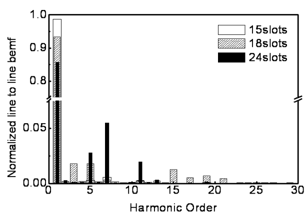

(a) line to line Back-EMF (b) harmonic component

Fig. 4 Comparisons of Back-EMF and THD results

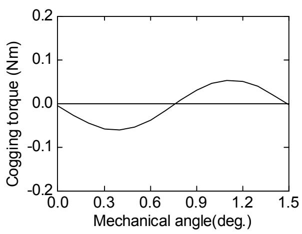

(a) 16p/15s mode

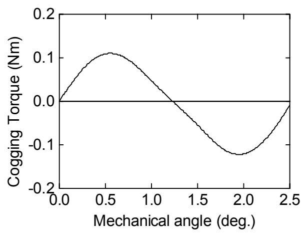

(b) 16p/18s model

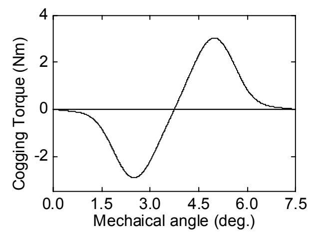

(c) 16p/24s model

Fig. 5 Comparison of cogging torque results

2.3.2 D-q axis Inductances

Inductance is another very important machine design parameters, which significantly affect the IPMSM output performances, such as the maximum torque and field weakening ability. According to the voltage equation given in the *d*-/*q*- axis equivalent circuits, the *d*-/*q*- axis inductances can be calculated with the help of FEA on the basis of Fig. 6 in steady state. The computation method is given in equation (4) and equation (5).

Fig. 7 shows the comparison of the d-/q- axis inductances and their saliency at rated current. Due to high winding factor, the 16p/15s design model shows high inductances L_d, and L_q. Especially *d*-axis inductance is high with low saliency ratio. Therefore, 16p/15s design model will generates lower reluctance torque and the larger magnetic torque compare to the 16p/24s design model.

$$L_d = \frac{\Psi_o \cos\alpha - \Psi_a}{i_d} \tag{4}$$

$$L_q = \frac{\Psi_o \sin\alpha}{i_q} \tag{5}$$

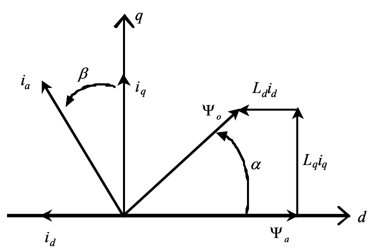

Fig. 6 Vector diagram in d-q frame

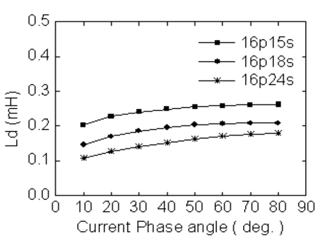

(a) 16p/15s mode

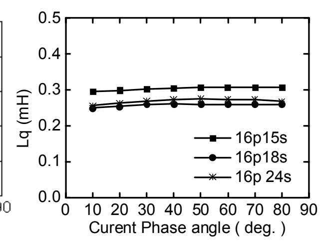

(b) 16p/18s model

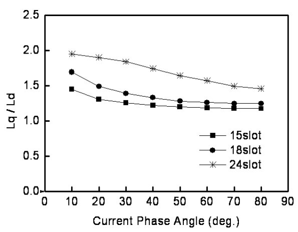

(c) 16p/24s model

Fig. 7 Comparison of L_d, L_q @rated current

2.4 Machine Characteristics

By performing d-q equivalent circuit, IPMSM performances in entire speed region can be predicted, as Fig. 8(a) shows. In constant torque region below 2000[rpm], maximum torque per ampere (MTPA) control is applied and maximum efficiency control is adopted in field weakening region. For generating required torque, the 16p/15s model needs minimum current in MTPA region, while 16p/18s does in field weakening region.

Then the torque characteristic is calculated by inputting an identical current with zero current phase angle β to three models, and their torque and torque ripple are compared as Fig. 8(b) shows. The 16p/15s model shows the largest torque with the smallest torque ripple. This comparison results shows that improvement of torque and torque ripple can be easily achieved by choosing appropriate pole/slot combination.

2.5 Radial Vibration Force

In this study, machine vibration is separately considered with the machine characteristics in IPMSM design. The vibration forces generate magnetic noise are mostly the radial forces [3]. The RVF due to the radial magnetic flux pressure acts on the stator causing vibrate and noise. RVF are attractive forces between the stator and rotor while tangential forces act on the rotor to produce torque. Generally, magnetic field of rotation machines can cancel out each other due to symmetric windings configuration, in contraste, the asymmetry windings configuration results in unbalanced magnetic field distribution, as Fig. 9 shows.

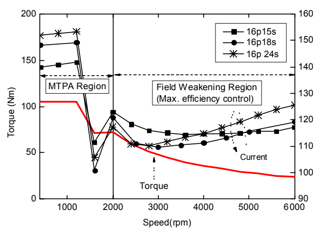

(a) input current according to speed

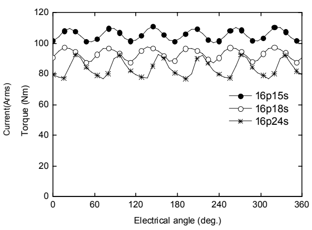

(b) output torque

Fig. 8 Comparison of motor performance

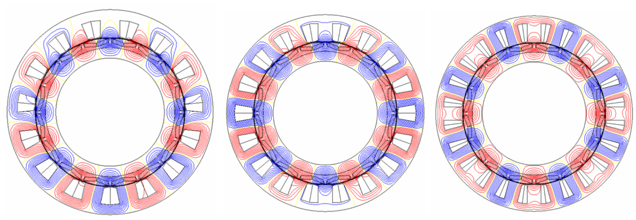

(a) 16p/15s mode (b) 16p/18s model (c) 16p/24s model

Fig. 9 Comparison of no-load flux distribution

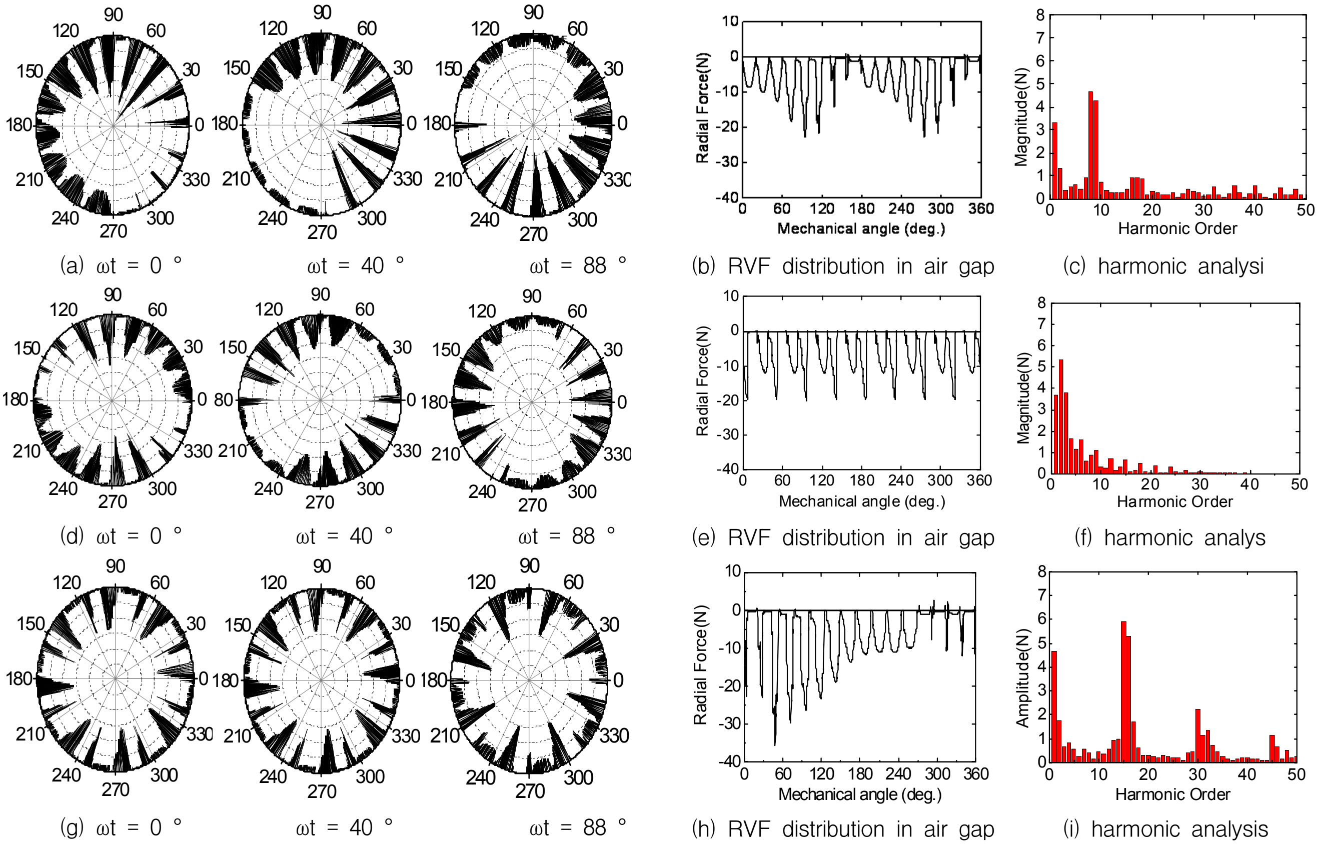

(a) ωt = 0 ° ωt = 40 ° ωt = 88 ° (b) RVF distribution in air gap (c) harmonic analysi

(d) ωt = 0 ° ωt = 40 ° ωt = 88 ° (e) RVF distribution in air gap (f) harmonic analys

(g) ωt = 0 ° ωt = 40 ° ωt = 88 ° (h) RVF distribution in air gap (i) harmonic analysis

Fig. 10 Comparison of radial vibration force (RVF) distribution in the air gap (@rated current, β=0°), and corresponded harmonic analysis

FEA is used to calculate the RVF. For this computation, only the radial component of the flux density is taken into account. The radial vibration force computation relies on the Maxwell Stress method, as:

$$\sigma(\theta,t)=\frac{1}{2\mu_o}B_n(\theta,t)^2 \tag{6}$$

where σ is RVF density, Θ is the angular coordinate, t is the time, μ_0 is the permeability of free space, and B_n is the radial component of the air gap flux density, respectively.

Fig. 10 shows results comparison of RVF distribution and correspond harmonic analysis in each model, that the 16p/15s model results of (a)~(c) show unbalanced RVF distributions, due to the asymmetric winding configuration, thereby serious noise and vibration can be expected. The results of (d)~(f) show a balanced symmetric RVF distribution in 16p/18s model, and it can be found that peak RVF is smaller than 16p/15s. Although the RVF distribution of 16p/18s model is symmetric, since high RVF components are distributed only 2-side along the air gap, relatively high noise and vibration are expected than 16p/24s model, which has RVF distribution as results of (g)~(h) shows, that the frequency of fundamental component is 4 times of 16p/18s model.

2.6 Results Summary and Analysis

From the present studies on the machine characteristics with RVF consideration, the compared results are listed in TABLE III. It can be concluded that the 16p/15s model should be avoided the IPMSM design due to its unbalanced RVF distribution in air gap, while under a trade-off consideration of winding factor, cogging torque, torque ripple, THD of Back-EMF, and balanced RVF distribution in air gap, the 16p/18s model is generally thought to be better design compare to the 16p/24s model for achieving low noise and vibration.

3. Conclusion

The paper presented a study on the machine characteristics in given IPMSM models with different pole/slot combinations, by comparing their characteristics of Back-EMF, inductances, cogging torque, torque performance, especially with separately consideration of vibration and noise by analyzing their radial vibration force. It is emphasized that an appropriate pole/slot combination choosing in IPMSM design helps to achieve

Table 3 Comparison of Parameters and Characteristics of Three IPMSM Models

	16p-15s model	16p-18s model	16p-24s model
Winding factor	0.951	0.931	0.866
Normalized Back-EMF	1.0	0.943	0.865
THD of Back-EMF (%)	0.866	0.97	4.82
Cogging torque(peak-peak) (Nm)	0.11	0.25	6.08
Torque ripple (%)	6	4.64	14.4
Inductance _ L_d (mH)	0.262	0.208	0.18
Saliency (L_q/L_d)	1.4	1.6	1.9
Parallel circuit	Should be avoided to prevent circulating current		available
RVF distribution	Unbalanced	Balanced	
* Noise Expectation	High	Medium	Low

the desired machine characteristics relative easily without detailed design.

Based on the introduced three IPMSM models, 16p/18s design model shows general better characteristics, that high winding factor and field weakening ability, low cogging torque, and torque ripple, in additional of balanced radial vibration force distribution. However, circulating current occurs when parallel circuit is used. Moreover, relations between RVF and noise and vibration need to be investigated in next work.

참 고 문 헌

[1] Shigeo Morimoto, Yoji Takeda, "Machine Parameters and Performance of Interior Permanent Magnet Synchronous Motors with Different Permanent Volume'', *Electrical Engineering in Japan*, vol. 131, No. 4, 2000.

[2] Freddy Magnussen, Chandur Sadarangani, "Winding Factors and Joule Losses of Permanent Magnet Machines with concentrated Windings", *Electric Machines and Drives Conference(IEMDC'03)*, vol. 1, pp. 333-339, June 2002.

[3] Takeda et al. Control schemes for PM motor and comparative characteristic of various rotor designs. Dengakuron; 114-D:662, 1994.

[4] Sung-Il Kim, Ji-Young Lee, Young-Kyoun Kim, Jung-Pyo Hong, Yoon Hur, Yeon-Hwan Jung, "Optimization for Reduction of Torque Ripple in Interior Permanent Magnet Motor by Using the Taguchi Method", *IEEE Transactions on Magnetics*, vol. 41, No. 5, May. 2005.

[5] Pia Salminen, Markku Niemelä and Juha Pyrhönen, Juhani Mantere, "Performance analysis of fractional slot wound PM motors for low speed applications", *IEEE Industry Applications Society Annual Meeting*, Oct., 2004.

저 자 소 개

방 량 (方 亮)

1980년 11월 18일생, 2003년 (China) Northeastern University 자동제어공학과 졸업, 2006년 창원대학교 대학원 전기공학과 졸업(석사), 2007년~현재 한양대학교 자동차 공학과 재학 (박사과정)

E-mail : fangliang@hanyang.ac.kr

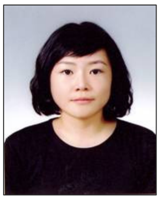

이 수 진 (李 壽 眞)

1984년 12월 18일생, 2007년 창원대학교 전기공학과 졸업, 2009년 한양대학교 대학원 자동차공학과 졸업(석사), 2010년~현재 한양대학교 자동차공학과 재학 (박사과정)

E-mail : issue@hanyang.ac.kr

이 병 화 (李 炳 華)

1980년 7월 05일생, 2006년 창원대학교 전기공학과 졸업, 2009년 한양대학교 대학원 자동차공학과 졸업(석사), 2009~현재 한양대학교 자동차공학과 재학 (박사과정)

E-mail : lbhwa@hanyang.ac.kr

홍 정 표 (洪 正 杓)

1959년 4월 17일생, 1983년한양대학교 전기공학과 졸업, 1985년 동 대학원 전기공학과 졸업(공학석사), 1985년 ~1990년 LG정밀(주) 중앙연구소 주임 연구원, 1990년~1992년 삼성전기(주) 종합연구소 선임 연구원, 1995년 동 대학원 전기공학과 졸업(공학박사), 1996년~2006년 창원대학교 전기공학과 부교수, 2006년~2008년 한양대학교 기계공학부 부교수, 2008년~현재 한양대학교 자동차공학과 교수, 2002년~현재 IEEE Senior member

E-mail : hongjp@hanyang.ac.kr